Liquid Crystals
Publication details, including instructions for authors and subscription information:
http://www.informaworld.com/smpp/title~content=t713926090

Hysteresis-free electro-optical switching in conductive ferroelectric liquid crystals: experiments and modelling

L. M. Blinov Corresponding author[ab]; S. P. Palto[b]; F. V. Podgornov[a]; H. Moritake[ac]; W. Haase[a]
[a] Institute of Physical Chemistry, Darmstadt University of Technology, 64287 Darmstadt, Germany [b] Institute of Crystallography, Moscow, Russia [c] Department of Electrical and Electronic Engineering, School of Electrical and Computer Engineering, National Defense Academy, Yokosuka, Kanagawa 239-8686, Japan

Online publication date: 19 May 2010

To cite this Article Blinov Corresponding author, L. M. , Palto, S. P. , Podgornov, F. V. , Moritake, H. and Haase, W.(2004) 'Hysteresis-free electro-optical switching in conductive ferroelectric liquid crystals: experiments and modelling', Liquid Crystals, 31: 1, 61 — 70
To link to this Article: DOI: 10.1080/02678290310001628528
URL: http://dx.doi.org/10.1080/02678290310001628528

LIQUID CRYSTALS, VOL. 31, NO. 1, JANUARY 2004, 61–70

Hysteresis-free electro-optical switching in conductive ferroelectric liquid crystals: experiments and modelling

L. M. BLINOV†‡*, S. P. PALTO‡, F. V. PODGORNOV†, H. MORITAKE†§ and W. HAASE†

†Institute of Physical Chemistry, Darmstadt University of Technology, Petersenstr.20, 64287 Darmstadt, Germany

‡Institute of Crystallography, RAS, 117333, Leninsky prosp. 59, Moscow, Russia

§Department of Electrical and Electronic Engineering, School of Electrical and Computer Engineering, National Defense Academy, 1-10-20 Hashirimidzu, Yokosuka, Kanagawa 239-8686, Japan

(*Received 5 February 2003; in final form 24 July 2003; accepted 18 August 2003*)

The hysteresis-free electro-optical switching, or so-called V-shaped, regime has been studied in a commercial ferroelectric liquid crystal (FLC) mixture having a smectic C* phase with a very small value of spontaneous polarization. The FLC was introduced into commercial EHC cells with thin aligning layers. In such cells V-shaped switching could be observed only at very low frequencies, less than 1 Hz. However, when the same material is strongly doped with a conductive impurity, its conductivity markedly increases and hysteresis-free switching is observed over a wide range of applied frequencies and voltages. Experimental results are in good agreement with computer modelling carried out as part of this work. The modelling takes into account all the important parameters of smectic C* FLC: non-polar anchoring conditions, possible bookshelf and chevron structures, the capacitance of the aligning layers and the conductivity of a FLC. The last two factors appear to be the most crucial for hysteresis-free switching in the smectic C* phase.

1. Introduction

Ferroelectric liquid crystals (FLCs) having a chiral smectic C* structure, possess an intrinsic polarity and can be driven to the 'on' and 'off' states by an external a.c. voltage. When a FLC structure is stabilized by surfaces, its electro-optical switching shows a threshold behaviour with a characteristic hysteresis [1]. However, several publications deal with a so-called 'V-shaped' or 'thresholdless' switching mode of ferroelectric and antiferroelectric (AFLC) liquid crystals following the pioneering work of Fukuda and co-workers [2]. In this case, the bookshelf alignment of smectic layers is provided by reasonably thick insulating films and the cell is placed between crossed polarizers with the smectic layer normal along the electric vector of incident light. When a triangular voltage waveform is applied to the cell, in a certain (usually narrow) range of field frequencies, the field-induced optical transmission curve acquires the form of the V-letter showing neither a threshold, nor hysteresis.

*Author for correspondence; e-mail: blinov@fis.unical.it

A mechanism for hysteresis-free V-shaped switching is still under discussion and many models have been suggested. Fukuda *et al.* [3, 4] relate the effect to a particular structure of the phase used (Langevin model). Rudquist *et al.* [5] suggest a 'block model' valid for any smectic C* FLC with self-interacting spontaneous polarization ($\mathbf{P}_s$). Very high $\mathbf{P}_s$ values are necessary in this model [6]. Other models [7, 8] relate V-shaped switching to strong polar anchoring of the FLC or AFLC to the polymer aligning layers. The important role of the capacitance of the aligning layers has been outlined by the Dublin group [9]. Finally, Čopič *et al.* have studied theoretically the influence of ions on the V-shaped electro-optical response [10]. It was assumed that the internal field in the FLC layer almost vanishes and that ions may be responsible for the anomalous hysteresis at very low frequencies. No experiment has been performed to support this view.

Recently we have reported theoretical and experimental results which show that hysteresis-free switching in the smectic C* phase can be observed over a wide frequency range determined, first of all, by parameters of a voltage divider formed by the capacitance of the

Liquid Crystals ISSN 0267-8292 print/ISSN 1366-5855 online © 2004 Taylor & Francis Ltd
http://www.tandf.co.uk/journals
DOI: 10.1080/02678290310001628528

aligning layers and the dynamic impedance of a FLC layer [11]. The FLC impedance itself depends on other properties of a FLC (such as $\mathbf{P}_s$, tilt angle, viscosity, anchoring conditions). In particular, a considerable increase in the frequency of the hysteresis-free switching with increasing FLC conductivity was predicted (by modelling). Experimentally, such a dependence has only been confirmed implicitly using either additional resistive elements [11] or a strong variation of conductivity with increasing temperature [12].

In the present paper we report on new results obtained for a strongly doped smectic C* FLC and compare these with those for the same basic material, but only slightly doped with the same impurity. We try to provide answers to the following questions: (i) should a V-shaped switching material be necessarily antiferroelectric or based on some frustrated ferroelectric structure as suggested in [3, 4]; (ii) must the spontaneous polarization indeed be large as it is assumed in the 'block' model [5, 6]; (iii) is the polar anchoring energy important for hysteresis-free switching as suggested in [7, 8]; (iv) how does the conductivity of FLC influence the frequency of hysteresis-free switching (the so-called hysteresis inversion frequency f_i introduced in [11]); (v) does the internal field in the FLC layer vanish in the V-shape regime as assumed in [10]; (vi) how does a chevron structure influence hysteresis-free switching; (vii) How does the simple analytical approach developed by Pikin [11] correspond to experiments and more advanced numerical calculations [13]?

Here we present experimental and computational results on electro-optical switching in a commercial FLC material (FELIX-015/000) having a very small $\mathbf{P}_s$ value, introduced into commercial EHC cells with thin aligning layers. In such cells no V-shaped switching is usually observed, at least, at frequencies exceeding $f \approx 1$ Hz. For $f > 1$ Hz V-shaped switching is still not observed when the FELIX-015/000 material is *lightly* doped with a well controlled conductive impurity. However, when the same material is *strongly* doped with the same impurity, its conductivity markedly increases and hysteresis-free switching is observed over a wide range of applied voltages and frequencies. This is key to obtaining a better understanding of the phenomenon and allows us to answer (at least, in a preliminary fashion) the questions posed above.

2. Experimental

2.1. *Materials and cells*

For the experiments we used Felix-015/000 (Clariant) ferroelectric mixture having the phase sequence: Iso 86°C N 83°C SmA 71°C SmC* −11°C SmX.

The parameters of the material measured by ourselves at 30°C are close to the manufacturer's data: tilt angle $\vartheta = 24°$, $\mathbf{P}_s = 9$–$10\,\mathrm{nC\,cm^{-2}}$, rotational viscosity $\gamma_\phi = 0.05\,\mathrm{Pa\,s}$, helical pitch $h > 100\,\mu\mathrm{m}$, optical anisotropy $\Delta n \approx 0.2$ (the temperature dependencies of ϑ, $\mathbf{P}_s$, and γ_ϕ can be found in a Clariant data sheet).

The commercial material has a residual electric conductivity σ in the range $(0.5\text{–}2) \times 10^{-9}\,\Omega^{-1}\mathrm{m}^{-1}$ (measured in a standard 2 μm thick EHC cell at $T = 30$°C with a triangular form voltage $U_{tr} = 5$ V at frequency $f = 1$ Hz). Its voltage and temperature behaviours were somewhat irregular. Upon doping, the electric properties of the material were stabilized. We doped it with tetracyanoquinondimethan (TCNQ) which is known to be one of the best electron acceptors. To this effect we dissolved both the FLC and TCNQ in acetone and obtained a uniform mixture after evaporation of the solvent at slightly elevated temperature (the homogeneity of TCNQ solutions in Felix-015/000 was checked under a microscope).

The concentration of the dopant was varied in the range of $c = 0.01$–1 wt%. The phase transition temperatures of the mixtures were measured using texture observations with an electric field applied to a cell. With an accuracy of the Mettler stage of about 1°C we observed no change in the phase transition temperatures up to $c = 1\%$. The spontaneous polarization and tilt angle measured at $T = 30$°C show no dependence on dopant concentration; however, the electro-optical studies reveal a 1.4 times increase in γ_φ for 1% TCNQ doped samples.

2.2. *Measurements*

We used standard 2 μm thick EHC cells of area $4 \times 4\,\mathrm{mm^2}$ with 30 ± 10 nm thick aligning polyimide layers (data of the manufacturer). They were filled with the FLC in the isotropic phase. The temperature dependences of the electrical current through the cells and the electro-optical response were measured using a set-up consisting of a rotating table with a temperature control, a He-Ne laser and a photomultiplier. The repolarization current and V-shaped response oscillograms were recorded by a digital oscilloscope HP54815A using triangular voltage pulses of frequency 0.2–100 Hz from a function generator HP33120a and voltage amplifier F20A (FLC Electronics, Sweden). From the current oscillogram we could extract the value of spontaneous polarization $\mathbf{P}_s$, the background dielectric constant ε and ohmic conductivity σ. Estimations of rotational viscosity were made using square-wave pulses. We also used an impedance meter and a lock-in amplifier technique for conductivity measurements at frequencies down to 0.5 Hz (with and without a bias d.c. voltage).

2.3. *Electric conductivity*

We shall limit ourselves to the comparison of two cells; namely, those filled with mixtures doped with small ($c=0.01$ wt%) and large ($c=1$ wt%) concentrations of TCNQ. In the SmC* phase both the slightly and strongly doped materials show optical textures with characteristic zig-zag defects indicating a chevron-type structure, see figure 1. Such chevrons spontaneously form on transition from the SmA phase to satisfy a strong planar anchoring at the electrodes.

The current oscillograms of the two cells taken at 30°C with a voltage $U_{tr}=5$ V at $f=1$ Hz are shown in figure 2. For small dopant concentration ($c=0.01\%$) the peak originating from $\mathbf{P}_s$ switching is well seen, and the calculated value of $\mathbf{P}_s=9\,\mathrm{nC\,cm^{-2}}$ coincides with the Clariant data. The steps of the current corresponding to the applied voltage peaks allow us to find the background dielectric constant (not related to the polarization switching), $\varepsilon=5.6$. The ohmic conductivity of the cell filled with $c=0.01\%$, calculated from the linear slope of the baseline under the peak is quite small, $G=0.003\,\mu$S (specific conductivity $\sigma=0.35\times10^{-9}\,\Omega^{-1}\,\mathrm{m}^{-1}$). Upon further doping the conductivity increases and reaches the value of $G=0.02\,\mu$S ($\sigma=2.5\times10^{-9}\,\Omega^{-1}\,\mathrm{m}^{-1}$) for $c=1\%$. In this case, the ionic current baseline is no longer linear and the polarization peak is strongly blurred, although no change in the electro-optical switching has been noticed.

The cell conductivity strongly depends on temperature, see figure 3. A strong increase in ionic conductivity, $\sigma=qn\mu$, with increasing temperature is expected because the ion concentration n grows due to the more efficient ionization of the neutral TCNQ–FLC complexes, and the ion mobility μ also grows due to a decrease in viscosity (q is the ionic charge). As we shall see later, the temperature increase in conductivity strongly correlates with the V-shaped switching electro-optical behaviour. Unfortunately the conductivity of the strongly doped cell decreases with time. The curves shown in figure 3 were measured almost three months later than the oscillogram shown in figure 2 and all other experiments and numerical calculations presented

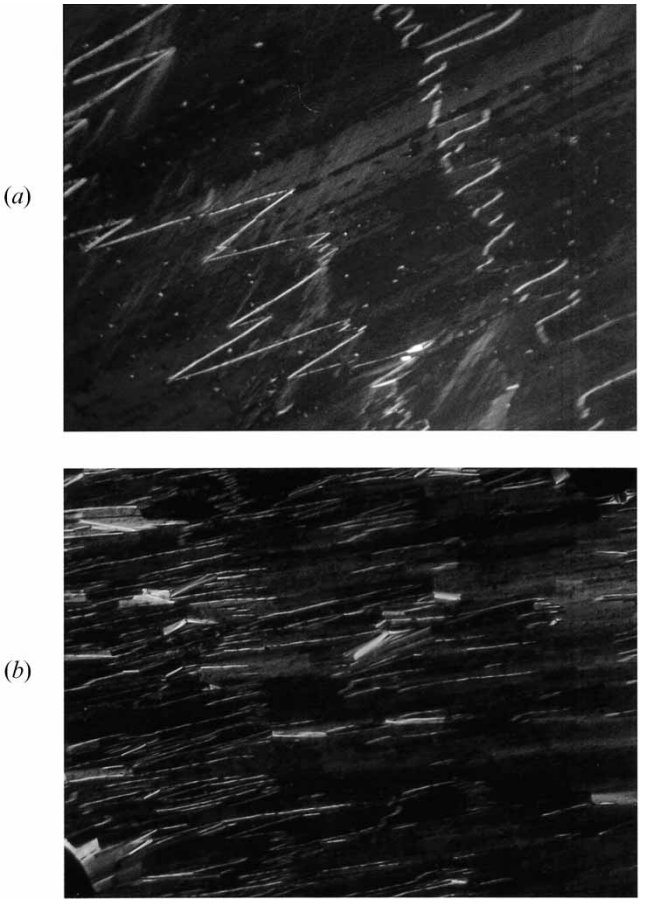

Figure 1. Optical textures of the SmC* phase observed in 2 μm thick cells filled with FELIX-015/000 mixture doped with (*a*) 0.01 wt% and (*b*) 1 wt% of TCNQ. Size of the area $0.66\times0.45\,\mathrm{mm^2}$.

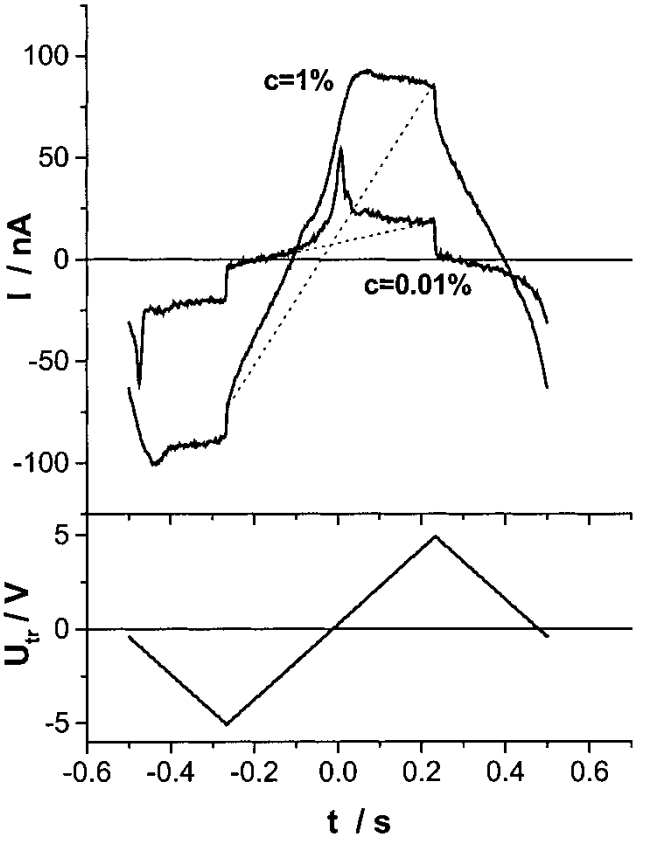

Figure 2. The current oscillograms of two FLC cells doped with small (0.01 wt%) and large (1%) concentrations of TCNQ. Data were taken at 30°C with a triangular voltage $U_{tr}=5$ V at $f=1$ Hz shown below the main plot.

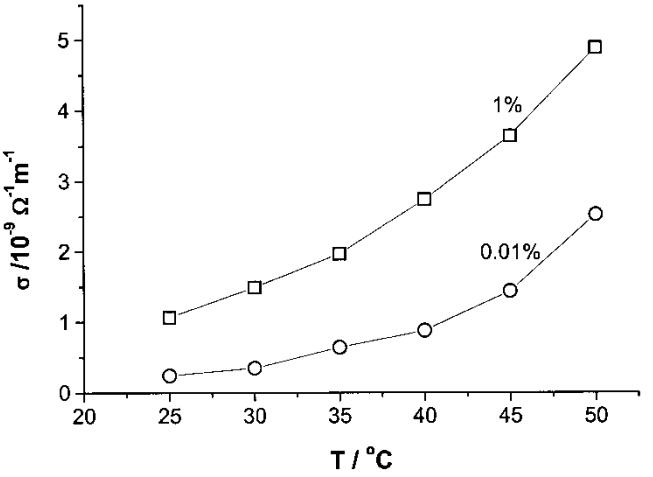

Figure 3. Temperature dependence of conductivity for slightly (0.01%) and strongly (1%) doped materials ($U_{tr}=5$ V, $f=1$ Hz).

later. This is why the cell conductivity at 30°C ($\sigma=1.5\times10^{-9}\,\Omega^{-1}\,m^{-1}$) is about half that found from figure 1. Nevertheless the qualitative picture is clear.

2.4. *Electro-optical properties*

The field-induced optical transmission $T(U_{tr})$ was measured with a cell placed between crossed polarizers in the symmetric angular position such that the transmission was maximum for maximum positive and negative fields. In this case, a $T(U_{tr})$ curve has either a 'W-shape' with two minima or 'V-shape' with one minimum. The coercive voltage U_c, defined as a half–width of the field hysteresis curve, is equal to half of the distance between the two minima of the W-letter. It is zero for hysteresis-free switching (V-shaped). The coercive field is frequency-dependent and we call the frequency at which it vanishes the hysteresis inversion frequency f_i, because for $f>f_i$ the hysteresis is normal but for $f<f_i$, its direction changes sign (abnormal hysteresis) [11]. The frequency f_i is very characteristic and important for understanding the phenomenon in question.

Figure 4 shows the dependence of the coercive voltage on frequency for the same two cells described previously ($T=30$°C). The zero line separates the areas of the abnormal (below) and normal (above) hysteresis. Such behaviour of $U_c(f)$ cannot be explained within the framework of the coercive field theory [14] developed without allowing for aligning layer properties (in [14] the coercive voltage does not change sign). For the cell filled with slightly doped material, figure 4 (*a*), hysteresis-free V shaped switching (crossings of the zero line) is observed at very low frequency. A typical oscillogram of the optical transmission taken at the

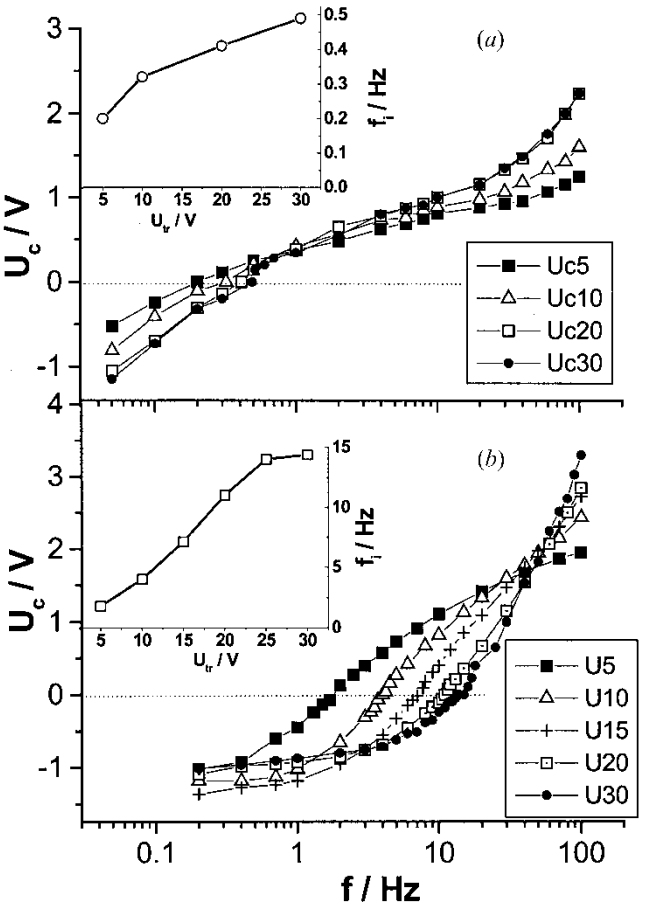

Figure 4. Frequency dependence of the coercive voltage for (*a*) slightly and (*b*) strongly doped materials. The amplitude of the applied triangular voltage is shown in the keys. Insets show the corresponding voltage dependences of the hysteresis inversion frequency.

hysteresis inversion frequency ($f_i=0.28$ Hz, $U_{tr}=\pm10$ V) is shown in figure 5 (the curve for $c=0.01\%$). The ratio of the field-induced and the zero field transmission (that is, a contrast) is small but this is expected because we deliberately use standard EHC cells manufactured for other purposes (mostly used for nematics) and the textures shown in figure 1 are far from ideal. We shall return to this problem later. The voltage dependence of f_i is shown in the inset to figure 4 (*a*): f_i is increasing with increasing voltage from 0.2 to 0.5 Hz. Therefore, in a standard frequency range ($f>1$ Hz) V-shaped switching is not seen.

The behaviour of the strongly doped material is qualitatively similar but all the curves are considerably shifted to a higher frequency, figure 4 (*b*). Now the coercive voltage becomes zero at frequencies more than an order of magnitude higher than in the case of the slightly doped material. This is exactly what was predicted in [11]. The inversion frequency f_i increases

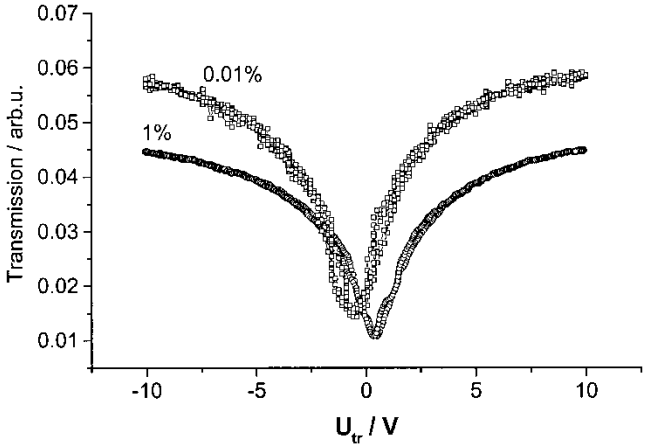

Figure 5. V-shaped optical transmittance for 2 μm thick cells filled with slightly ($c=0.01$ wt%) and strongly doped FELIX-015/000 mixtures at hysteresis inversion frequencies, $f_i=0.28$ Hz for $c=0.01$ wt% TCNQ and $f_i=3.5$ Hz for $c=1$ wt% TCNQ ($T=30°C$, $U_{tr}=\pm 10$ V).

from 2 to 14 Hz with increasing voltage. This dependence is shown in the inset to figure 4 (*b*) and will also be discussed in the next section. The optical transmission curve taken at $f_i=3.5$ Hz, is shown in figure 5 for a triangular voltage $U_{tr}=\pm 10$ V.

The voltage dependences of the inversion frequency at three different temperatures are shown in figure 6. For a small concentration of ions (*a*) ($c=0.01\%$, curves for 30°C and 40°C) the inversion frequency is low (less than 0.6 Hz) and almost voltage-independent. With increasing conductivity, f_i increases and becomes voltage-dependent. For the slightly doped material it reaches 2.5 Hz at $U_{tr}=\pm 30$ V and 50°C. This tendency is even more pronounced for the strongly doped material, figure 6 (*b*). The maximum frequency at which V-shaped switching is observed is 27 Hz at $U_{tr}=\pm 30$ V and 48°C. A strong temperature dependence at $U_{tr}=\pm 5$ V correlates with the strong temperature dependence of specific conductivity shown in figure 3. From this experiment it is quite evident that for appropriately doped materials one can obtain V-shaped switching at fairly high frequencies, even using thin aligning layers and for a low spontaneous polarization. However, the electro-optical performance will be better for thicker layers, better texture quality (as already shown in [11]) and a higher $\mathbf{P}_s$ (see later).

3. Modelling and discussion

3.1. *Modelling procedure*

Our modelling technique and its application to V-shaped electro-optical switching in the smectic C* phase has been briefly outlined in [11], and described in detail in [13, 15]. Its application to different electro-optical effects (including V-shaped switching) was reported at

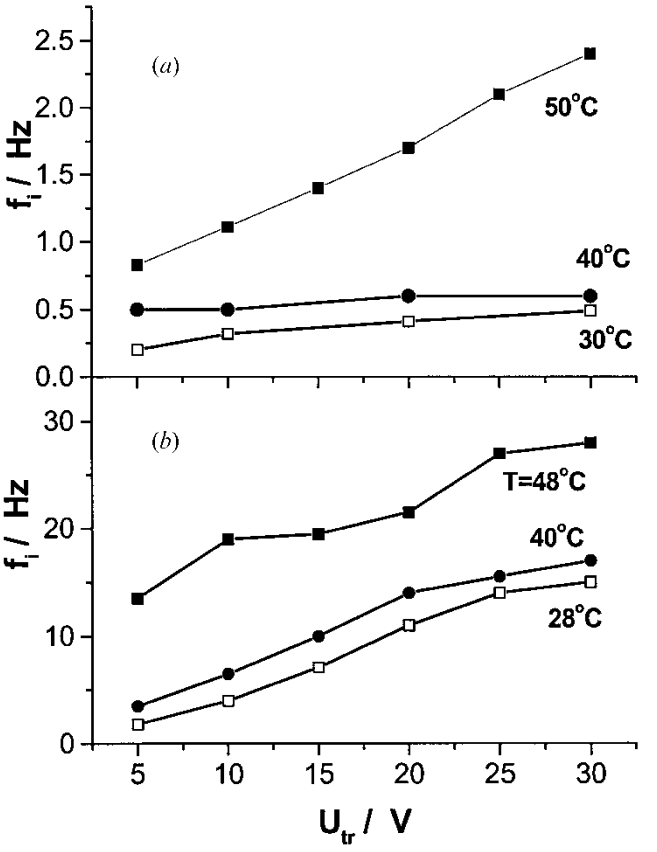

Figure 6. Voltage dependences of the inversion frequency at different temperatures. (*a*) slightly doped material ($c=0.01$ wt% TCNQ); (*b*) strongly doped material ($c=1$ wt% TCNQ). Cell thickness 2 μm.

the Edinburgh ILCC 2002 and will be published elsewhere [16, 17]. Recently the software has been developed to take a simple chevron structure into account. Here we just overview the most important points.

The hysteresis inversion frequency and a particular form of the optical transmission $T(U_{tr})$ curve depend on parameters of the FLC and aligning layers of capacitance C_p in a very complex way. To simulate this effect we have solved two sets of equations: (1) dynamic equations for the director $n(t, z, U)$ coupled with electric current equations; (2) Maxwell equations for calculations of the optical transmission $T(t,U)$ for different polarization, wavelength and coherency of light incident onto a cell.

The problem is simplified in the sense that the director distortion is treated as unidimensional (along the *z*-axis) and flow is ignored. Where necessary, the following contributions may be taken into account in the Euler–Lagrange equations for the chiral SmC* phase: (i) a visco-elastic term including molecular tilt

angle Θ in the smectic layers, three rotational viscosity coefficients γ_i, three Frank moduli K_{ii}, a layer compressibility modulus K_4 and spontaneous twist and bend coefficients; (ii) electric terms including spontaneous polarization $\mathbf{P}_s$, two dielectric tensor components ε_i and an applied voltage of arbitrary form; (iii) a surface term including variable pretilt angles ϑ_s, azimuthal W_a and zenithal W_z anchoring energies; (iv) it is also possible to vary the angle β between the smectic layer normal and the normal to the sandwich cell: e.g. $\beta=\pi/2$ for the bookshelf geometry, $\beta<\pi/2$ or $\beta>\pi/2$ for tilted layers while a chevron can be modelled by setting $\beta=\pi/2+\vartheta$ over a half of the cell thickness and $\beta=\pi/2-\vartheta$ over the other half (for details see [13]). During switching the chevron configuration was considered to be stable and the electric properties of the chevron interface were taken because the dielectric displacement includes polarization effects. However, the possible inhomogeneity of the free charge distribution at the chevron interface is not accounted for.

In the equations for the electric current, the electric properties (capacitance and conductivity) of both aligning layers and the FLC can be taken into account (the conductivity of a FLC was taken as a constant and the diffusion current was neglected). The applied field may have an arbitrary form. The optical transmission $T(t,U)$ is calculated using the Berreman matrix method and a new algorithm described in [15]. At this stage, properties of all optical elements (light source, polarizers, conductive glasses, aligning layers, FLC layer thickness d) were taken into account.

In the present work, in addition to variable parameters (amplitude and frequency of the applied voltage, conductivity G of the cell, in some cases viscosity and polarization) we used two groups of fixed parameters. The parameters of the first group are known from independent measurements. At $T=30^\circ$C these are: cell thickness $d=2\,\mu$m, cell area $16\,\text{mm}^2$, capacitance of two aligning layers $C_p=8.9\,$nF, tilt angle $\vartheta=24^\circ$, polarization $\mathbf{P}_s=9\,\text{nC}\,\text{cm}^{-2}$, rotational viscosity (all three components) $\gamma_0=0.32$ and $0.45\,$Pa s respectively for dopant concentration 0.01% and 1%, both components of the dielectric tensor $\varepsilon=5.6$, inverse pitch $0.01\,\mu\text{m}^{-1}$, optical anisotropy at $\lambda=632.8\,$nm $\Delta n=0.155$; the chevron structure was fixed by setting $\vartheta_1=90-\vartheta=66^\circ$ and $\vartheta_2=90+\vartheta=114^\circ$. The parameters of the second group were taken from the literature for typical FLC materials. These are: three Frank elastic moduli $K_{ii}=10\,$pN, ordinary index of refraction $n_o=1.53$, pretilt $\vartheta_s=4^\circ$ on both electrodes, anchoring energy $0.05\,\text{mJ}\,\text{m}^{-2}$ (azimuthal) and $0.5\,\text{mJ}\,\text{m}^{-2}$ (zenithal) on both electrodes, compressibility modulus was fixed at $K_4=1\,$MPa to make the calculation faster (in fact, K_4 is considerably larger [16], but far from the ferroelectric transition it does not influence the results).

Therefore, our modelling includes the most important parameters of the FLC materials and cells with few exceptions. In fact, we neglect spatial domains (due to the one-dimensional treatment), flow of mass, field dependence of conductivity and polar anchoring. However, we would like to stress that we are only interested in conventional smectic C* materials; all equations were formulated for the smectic C* phase and, in this modelling, we used only realistic parameters of modern materials.

3.2. *Current oscillograms*

An example of the calculated oscillogram of the electric current is shown in figure 7. It is an attempt to model the experimental oscillograms shown in figure 2. We model the cell texture with a symmetric chevron structure: the wall between the two tilted structures is located exactly in the middle of the cell. For the slightly doped material ($G=0.003\,\mu$S) the experimental and calculated oscillograms are very similar: the height and the slope of the background are the same, the area under the $\mathbf{P}_s$ peak is also the same, $\mathbf{P}_s=9\,\text{nC}\,\text{cm}^{-2}$. However, the calculated peak is narrower than the experimental one. We believe that it is related to the non-ideal texture of our experimental cell: when the current peak coming from $\mathbf{P}_s$ is calculated for the bookshelf geometry, it is even narrower than that for the chevron structure shown in the oscillogram.

The discrepancy between experiment and calculations is more serious for the strongly doped material.

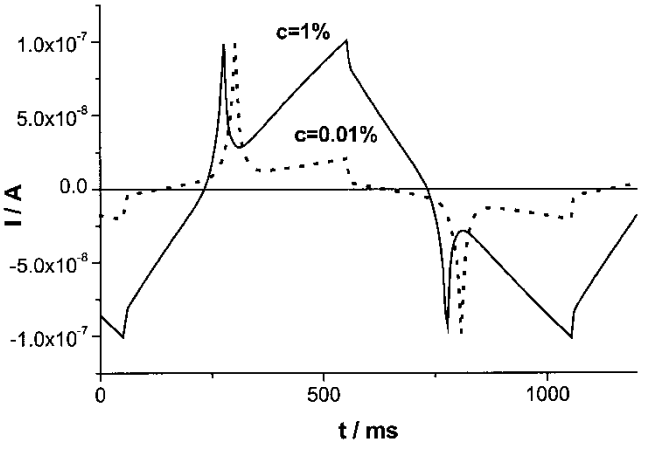

Figure 7. Calculated current oscillograms for two FLC cells filled with slightly conductive ($G=0.003\,\mu$S) and strongly conductive ($G=0.02\,\mu$S) materials. Other parameters correspond to FELIX-015/000 mixture at 30°C. Calculations have been made for a symmetric chevron structure and triangular voltage $U_{tr}=5\,$V at $f=1\,$Hz.

Experimentally (figure 2) the conductivity current is no longer linear with voltage and the $\mathbf{P}_s$-related current peak is completely blurred. Our modelling does not show this, the calculated current–voltage curve is linear and the $\mathbf{P}_s$-related current peak on the steep background is still sharp. In our opinion, two factors may be responsible for such discrepancies. First, when the electric field is applied to the real cell filled with strongly doped material, the ions are no longer distributed uniformly over the cell thickness as suggested in [10] and this may modify the current pulse shape (in our model this effect is not taken into account). The other reason may be even more serious: backflow effects, which are well known for nematic liquid crystals, play an important role in the smectic C* phase, especially in the case of strong conductivity, and such hydrodynamic effects are not taken into account in our software.

3.3. *Coercive field and V-shaped switching*

The calculated frequency dependence of the coercive voltage for the strongly conductive FLC material ($G=0.02\,\mu$S) having a symmetric chevron structure is shown in figure 8. We have to compare it with experimental curves shown in figure 4 (*b*). In both cases, the coercive voltage passes the zero point in the frequency range centred about 4–5 Hz, and the shape of the curves in both cases is similar. However, the calculated voltage dependence of the hysteresis inversion frequency is weaker than the experimental one, compare insets to figures 4 (*b*) and 8 (upper curve). Experimentally we observe hysteresis-free switching in the range $f_i \approx 2$–15 Hz, calculation results in $f_i \approx 3.5$–5.3 Hz.

When the calculations are carried out for the bookshelf geometry the hysteresis inversion frequency falls within the range $f_i \approx 0.9$–3 Hz, see the lower curve in the inset to figure 8. It is an interesting result because general opinion is that V-shaped switching is hardly compatible with chevron structures but, in fact, f_i is higher for a chevron structure. In both the bookshelf and chevron textures the calculated f_i is voltage-dependent. Such a dependence comes from the voltage dependence of the switching time $\tau = \gamma_\phi / PE$ because it follows from the analytical solution of Pikin [11] and our previous experiments [11] which have shown that the V-shaped regime is promoted to higher frequencies by decreasing γ_ϕ and increasing $\mathbf{P}_s$ (see also figure 11 later).

The form of the calculated V-curve for the bookshelf texture is much narrower than that for the chevron texture, and both of them are narrower than the experimental ones, compare figures 2 and 9. The reason for this is, most probably, a serious inhomogeneity of the experimental textures prepared using standard EHC cells. Therefore, a voltage necessary to reach the maximum transmission (so-called saturation voltage) is higher for the chevron or other inhomogeneous structures than that for the bookshelf texture.

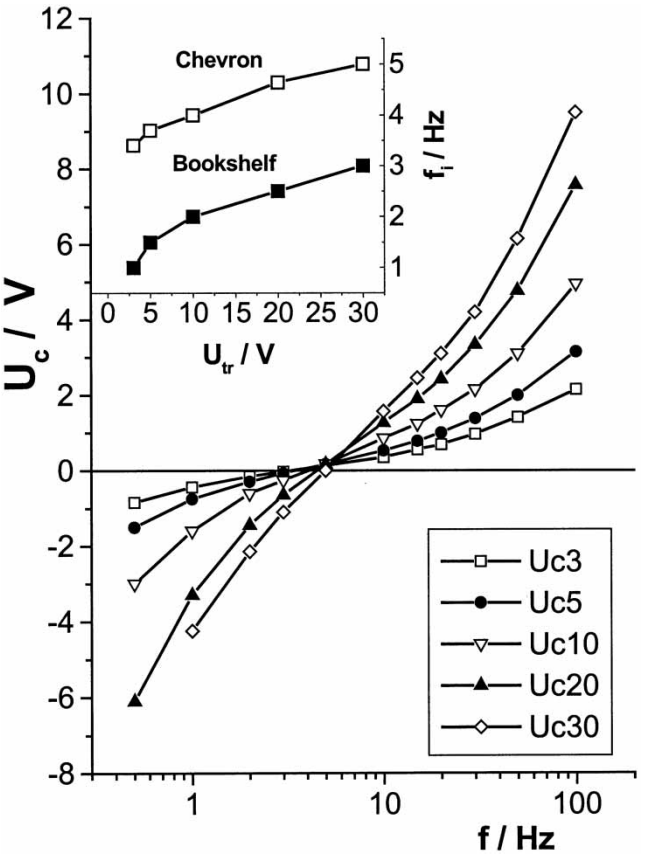

Figure 8. Calculated frequency dependence of the coercive voltage for the strongly conductive FLC material ($G=0.02\,\mu$S) having a symmetric chevron structure. The amplitude of the applied triangular voltage is shown in the keys. The inset shows the corresponding voltage dependences of the hysteresis inversion frequency for the chevron structure in comparison with the bookshelf structure (other parameters are the same).

3.4. *Calculated* f_i *dependence on conductivity and spontaneous polarization*

Experimentally, it is difficult to change one parameter while not influencing the others. However, it is easy to do so by modelling. Below we vary separately the most important parameters responsible for hysteresis-free switching: cell conductivity G, spontaneous polarization $\mathbf{P}_s$ and rotational viscosity γ_ϕ. (The role of the capacitance of the aligning layers C_p which is also of great importance was analysed earlier. It has been

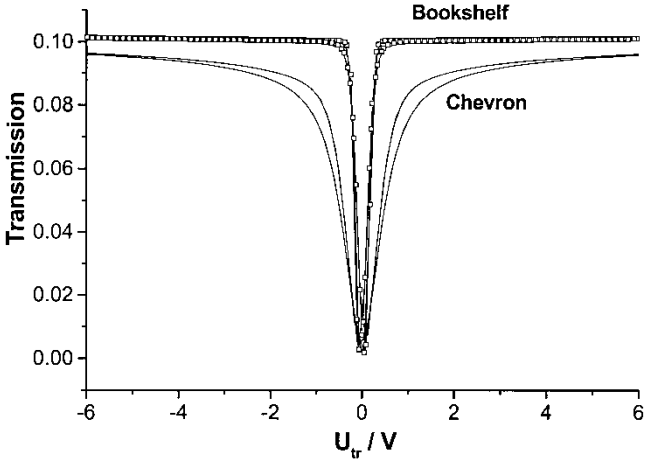

Figure 9. Calculated V-shaped optical transmittance for two 2 μm thick FLC cells filled with the same strongly conductive ($G=0.02\,\mu S$) material but having different textures, bookshelf and chevron. Other parameters correspond to FELIX-015/000 mixture at 30°C. At $U_{tr}=\pm 10\,V$ hysteresis inversion frequencies $f_i=2Hz$ and 4 Hz for the bookshelf and chevron structures, respectively.

shown that decreasing C_p dramatically increases f_i [11, 17]).

The calculated frequency dependences of the coercive voltage for FLC materials having a symmetric chevron structure and different cell conductivity G are shown in figure 10. The other parameters are the same as before. As expected, with increasing conductivity the zero points are shifted to higher frequencies.

There is, however, a very interesting curve for $G=0$. It does not cross the abscissa, but asymptotically goes to zero upon decreasing frequency. This means that, strictly speaking, hysteresis-free switching for non-conductive smectic C* materials can be observed only at zero frequency. From the practical point of view, at frequencies up to a few Hz the coercive field can be small enough to provide a quasi-V-shaped switching even in a non-conductive FLC. However, in order to obtain V-shaped switching at enhanced frequencies a FLC material (at least with low $\mathbf{P}_s$) should be conductive.

The dependence of the hysteresis inversion frequency on the square root of conductivity is shown in the inset in figure 10 for both chevron and bookshelf textures. The abscissa is selected in order to check a prediction of the simple analytical theory developed by Pikin [11]. Indeed, the functions f_i ($G^{1/2}$) are almost linear, as predicted. The same theory correctly describes the $f_i(C_p)$ dependence. For small $\mathbf{P}_s$ it also predicts a linear increase in f_i with increasing spontaneous polarization

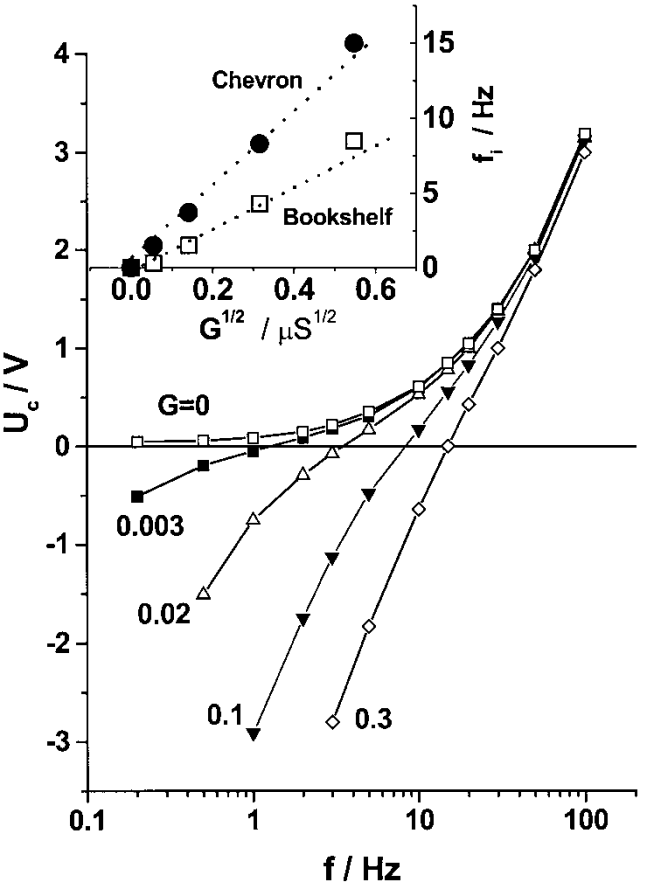

Figure 10. Calculated frequency dependence of the coercive voltage for FLC materials having a symmetric chevron structure and different cell conductivity G ($U_{tr}=\pm 5\,V$, cell thickness 2 μm, area 16 mm^2, other parameters correspond to FELIX-015/000 mixture at 30°C). The inset shows the corresponding dependences of the hysteresis inversion frequency for the chevron structure in comparison with the bookshelf structure on the square root of conductivity (other parameters for the two curves are the same).

and a decrease in f_i with increasing rotational viscosity. Now we can verify that analytical result by modelling.

In this case, we model a cell with the same geometry as before, a bookshelf texture and parameters more suitable for high frequency V-shaped switching. The capacitance of aligning layers and conductivity are close to the optimum, $C_p=5\,nF$, $G=0.015\,\mu S$, rotational viscosity values are typical, $\gamma_0=0.25$ and 0.6 Pa s. The calculated dependences of the hysteresis inversion frequency on the spontaneous polarization for the two γ_0 are shown in figure 11. Indeed, for $\mathbf{P}_s<40\,nC/cm^2$, f_i grows almost linearly with P_s and then somewhat faster. In this sense, high values of P_s are preferable for V-shape switching as discussed in [5], however, the hysteresis-free switching is also possible for very small

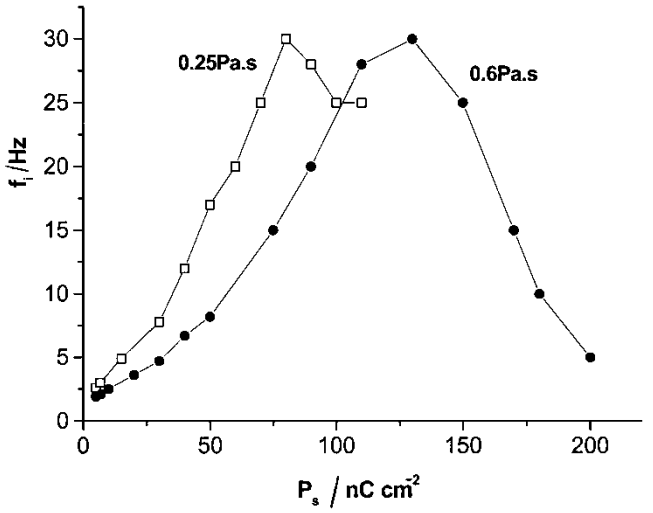

Figure 11. Calculated dependences of the hysteresis inversion frequency on the spontaneous polarization for a FLC cell with the bookshelf structure. The material and cell parameters are: $K_{ii}=10\,\mathrm{pN}$, $\vartheta=24^\circ$, $\varepsilon_{ii}=3.5$, $G=0.015\,\mu\mathrm{S}$, $C_\mathrm{p}=5\,\mathrm{nF}$, $d=2\,\mu\mathrm{m}$, $\mathrm{A}=16\,\mathrm{mm}^2$, $U_\mathrm{tr}=\pm 10\,\mathrm{V}$. The two curves differ by the values of rotational viscosity γ_0 indicated (note, that $\gamma_\phi=\gamma_0\sin^2\vartheta$). For other, less important parameters see the text.

P_s. Low viscosity is also favorable for fast V-shape regime in the range of $P_\mathrm{s}<100\mathrm{nC/cm}^2$. However, on further increasing P_s the curves reach their maxima and then f_i decreases. The reason for this is not clear, but such a tendency should be taken into account when tailoring new materials for the V-shape effect.

3.5. *Comment on the shape of the field on a FLC layer*

The software used allows us to follow the shape of the voltage on the FLC layer $U_\mathrm{LC}(f)$ on varying the amplitude and frequency of the voltage applied to a cell $U_\mathrm{tr}(f)$. According to [5, 6, 8] and the simplest analytical model [11] the V-shaped regime occurs when the field within the FLC layer is small and almost uniform. Our modelling shows that, for materials with high $\mathbf{P}_\mathrm{s}$, the form of U_LC does change when the frequency of U_tr is close to f_i; indeed, far from f_i, U_LC has the same triangular shape as U_tr, but close to the inversion frequency U_LC vanishes within some time interval close to the zero point of U_tr. At the same time the repolarization current peak has a very flat top. Within one voltage period, T_tr, each of the two zero field time intervals takes some 5–10% of T_tr. For materials with small $\mathbf{P}_\mathrm{s}$ the voltage U_LC remains triangular for any frequency near f_i, with some phase shift with respect to the external voltage U_tr. Therefore the V-shaped regime, in general, does not require zero U_LC that is a zero integral of the electric field over the FLC layer thickness.

4. Conclusion

In conclusion, we have carried out the measurement and modelling of the current oscillograms and frequency and voltage dependences of the hysteresis inversion frequency in a conventional smectic C* FLC. The results allow us to obtain at least preliminary answers to the questions posed in the Introduction.

(i) Should a material be necessarily antiferroelectric or based on some frustrated ferroelectric structure? We believe, it should not, because the V-shaped switching regime can be observed and optimized for typical smectic C* ferroelectric liquid crystals over a wide range of material parameters.

(ii) Must the spontaneous polarization indeed be large as it is assumed in the 'block' model? Evidently it need not, because the V-shape regime has been experimentally studied in a material with very small $\mathbf{P}_\mathrm{s}=9\,\mathrm{nC\,cm}^{-2}$, and the modelling shows that $\mathbf{P}_\mathrm{s}$ can be even smaller. However, high $\mathbf{P}_\mathrm{s}$ promotes the V-shaped regime to higher frequencies.

(iii) Is the polar anchoring energy important for hysteresis-free switching? Since in standard cells without any effort to prepare a special alignment, we observe V-shaped switching, most probably special anchoring is not very important. The problem of polar anchoring was not studied explicitly. In our calculations, however, we varied both types of Rapini-form anchoring energy (azimuthal and zenithal) over a wide range, from 0.01 to $0.5\,\mathrm{mJ\,m}^{-2}$, and saw no substantial effect on V-shaped switching.

(iv) How does the conductivity of an FLC influence the frequency of hysteresis-free switching? Both experimental data and modelling show a dramatic influence of conductivity on hysteresis-free switching: the higher the conductivity the higher is the hysteresis inversion frequency. The modelling shows that for a non-conducting FLC V-shaped switching is allowed only at zero frequency.

(v) Should the internal field in the FLC layer vanish in the V-shape regime as assumed in [11]? Generally not, but for high $\mathbf{P}_\mathrm{s}$ materials a dramatic decrease of the voltage on the FLC layer is modelled.

(vi) How does a chevron structure influence hysteresis-free switching? The field behaviours of the chevron and the bookshelf structures

have been compared by computer modelling. It was concluded that the V-shape regime can be observed in both cases, however, in the case of chevrons the saturation voltage is considerably larger. At the same time, the hysteresis inversion frequency is higher for the chevron structure.

(vii) How does the simple analytical approach developed in [11] correspond to experiment and more advanced numerical calculations? The analytical approach correctly describes the dependences of the hysteresis inversion frequency on most of the important material and cell parameters, such as spontaneous polarization (for low $\mathbf{P}_s$), rotational viscosity, conductivity and capacitance of the aligning layers.

Finally, we would like to stress that our results are related to conventional smectic C* FLC, conventional types of cells and conventional material parameters. In this case, as was noted, we do not see the possibility of obtaining hysteresis-free switching over a wide frequency range without the use of capacitive insulating layers and a conductive FLC. The role of these layers is to modify the field in the liquid crystal layer and eliminate surface-stabilized bistability. In our opinion, bistability and hysteresis-free switching are two sides of the same coin. In fact, and this is very important, bistability and hysteresis are not intrinsic, fundamental properties of the smectic C* phase because both come from the FLC interaction with a surface.

This does not mean that some other phases cannot show hysteresis-free switching. For example, the electroclinic effect in the smectic A* phase never shows hysteresis. The same can be true for the so-called frustrated smectic C* with Langevin-type switching [3, 4], or probably for the so-called de Vries smectics. However, such phases should be described by fundamental equations different from those used for the smectic C* description and have not been discussed here.

The authors are grateful to S.A.Pikin, for many discussions. W.H. thanks Volkswagen Foundation and Sony International (Europe) GmbH for financial support. L.M.B. and S.P.P. acknowledge financial support from the Russian Fund for Basic Research (grant no.03-02-17288); S.P.P. also thanks Russian Science Support Foundation.

References

[1] Lagerwall, S. T., 1999, *Ferroelectric and Antiferroelectric Liquid Crystals* (Weinheim: Wiley-VCH).
[2] Inui, S., Iimura, N., Suzuki, T., Iwane, H., Miyachi, K., Takanishi, Y., and Fukuda, A., 1996, *J. mater. chem.*, **6,** 671.
[3] Chandani, A., Cui, Y., Seomun, S. S., Takanishi, Y., Ishikawa, K., Takezoe, H., and Fukuda, A., 1999, *Liq. Cryst.*, **26,** 151, 167.
[4] Takeuchi, M., Chao, K., Ando, T., Matsumoto, T., Fukuda, A., and Yamashita, M., 2000, *Ferroelectrics*, **246,** 1.
[5] Rudquist, P., Lagerwall, J. P. F., Buivydas, M., Gouda, F., Lagerwall, S. T., Clark, N. A., Maclennan, J. E., Shao, R., Coleman, D. A., Bardon, S., Link, D. R., Natale, G., Glaser, M. A., Walba, D. M., Wang, M. D., and Chen, X.-H., 1999, *J. mater Chem.*, **9,** 1257.
[6] Clark, N. A., Coleman, D., and Maclennan, J. E., 2000, *Liq. Cryst.*, **27,** 985.
[7] Mottram, N. J., and Elston, S. J., 2000, *Phys. Rev. E.*, **62,** 6787.
[8] Čopič, M., Maclennan, J. E., and Clark, N., 2002, *Phys. Rev. E.*, **65,** 021 708.
[9] Panarin, Yu., Panov, V., Kalinovskaya, O. E., and Vij, J. K., 2000, *Ferroelectrics*, **246,** 35.
[10] Čopič, M., Maclennan, J. E., and Clark, N., 2001, *Phys. Rev. E.*, **63,** 031 703.
[11] Blinov, L. M., Pozhidaev, E. P., Podgornov, F. V., Pikin, S. A., Palto, S. P., Sinha, A., Yasuda, A., Hashimoto, S., and Haase, W., 2002, *Phys. Rev. E.*, **66,** 21 701.
[12] Blinov, L. M., Pozhidaev, E. P., Podgornov, F. V., Sinha, A., and Haase, W., 2002, *Ferroelectrics*, **277,** 3.
[13] Palto, S. P., 2003, *Kristallografia*, **48,** 145.
[14] Reynarts, C., and de Vos, A., 1991, *Ferroelectrics*, **113,** 432.
[15] Palto, S. P., 2001, *JETP*, **92,** 552.
[16] Palto, S. P., Blinov, L. M., Podgornov, F. V., and Haase, W. *Mol. Cryst. liq. Cryst*. (submitted).
[17] Blinov, L. M., Palto, S. P., Andreev, A. L., Pozhidaev, E. P., Podgornov, F. V., and Haase, W. *Mol. Cryst. liq. Cryst*. (submitted).